Mon. Not. R. Astron. Soc. **000**, 1–5 (2008) Printed 17 June 2008 (MN LaTeX style file v2.2)

arXiv:0806.2815v1 [astro-ph] 17 Jun 2008

The very massive binary NGC3603-A1

O. Schnurr[1,2⋆], A. F. J. Moffat[1], N. St-Louis[1], J. Casoli[1,3], and A.-N. Chené[1,4]

[1] *Dépt. de Physique , Université de Montréal, C. P. 6128, succ. centre-ville, Montréal (Qc) H3C 3J7, and Centre de Recherche en Astrophysique du Québec, Canada*
[2] *Dept. of Physics and Astronomy, University of Sheffield, Hicks Building Hounsfield Road, Sheffield S3 7RH, United Kingdom*
[3] *Ecole Normale Supérieure, 45, rue d'Ulm, 75230 Paris Cédex 05, France*
[4] *Herzberg Institute of Astrophysics, 5071 West Saanich Road, Victoria (BC) V9E 2E7, Canada*

Version 17 June 2008

ABSTRACT

Using VLT/SINFONI, we have obtained repeated AO-assisted, NIR spectroscopy of the three central WN6ha stars in the core of the very young (~ 1 Myr), massive and dense Galactic cluster NGC3603. One of these stars, NGC3603-A1, is a known 3.77-day, double-eclipsing binary, while another one, NGC3603-C, is one of the brightest X-ray sources among all known Galactic WR stars, which usually is a strong indication for binarity. Our study reveals that star C is indeed an 8.9-day binary, although only the WN6ha component is visible in our spectra; therefore we temporarily classify star C as an SB1 system. A1, on the other hand, is found to consist of two emission-line stars of similar, but not necessarily of identical spectral type, which can be followed over most the orbit. Using radial velocities for both components and the previously known inclination angle of the system, we are able to derive absolute masses for both stars in A1. We find $M_1 = (116 \pm 31) M_\odot$ for the primary and $M_2 = (89 \pm 16) M_\odot$ for the secondary component of A1. While uncertainties are large, A1 is intrinsically half a magnitude brighter than WR20a, the current record holder with 83 and 82 $M_\odot$, respectively; therefore, it is likely that the primary in A1 is indeed the most massive star weighed so far.

Key words: binaries: general – stars: evolution – stars: fundamental parameters

1 INTRODUCTION

While models maintain that in the early Universe, the first-generation of stars were very massive and reached masses between 100 and 1000 M$_\odot$ (e.g. Nakamura & Umemura 2001; Schaerer 2002), it is generally accepted that under present-day conditions, relatively fewer massive stars are formed, i.e. that the initial-mass function (IMF) is much steeper and, more importantly, has a cut-off occurring around 150 M$_\odot$ (Weidner & Kroupa 2004; Figer 2005). So far, however, whenever Keplerian orbits of binary systems are used to weigh stars – the only way to obtain reliable, least model-dependent masses –, measured masses fall short by almost a factor of two with respect to the putative cut-off. Currently, stars with the highest known masses are both WN6ha components of the Galactic WR binary WR20a, with 83 and 82 M$_\odot$, respectively (Rauw et al. 2004; Bonanos et al. 2004), and the O3f/WN6 star in the Galactic binary WR21a with a minimum mass of 87 M$_\odot$ (Gamen et al. 2008). Significantly more massive stars, however, have so far remained elusive.

A most remarkable result that has emerged from the search for very massive stars is, however, that the highest Keplerian masses are *not* found among absorption-line O-type stars – rather, masses of these stars remain below ~ 60 M$_\odot$ (e.g. Lamontagne et al. 1996; Massey et al. 2002) –, but among Wolf-Rayet (WR) stars, more precisely among the so-called WN5-7ha (or WN5-7h) stars, an extremely luminous and hydrogen-rich subtype of the nitrogen-sequence WR stars. Contrary to classical WR stars, which are identified with bare, helium-burning cores of evolved massive stars, theoretical work confirms that these luminous WN5-7ha stars are hydrogen-burning, unevolved objects (de Koter et al. 1997; Crowther & Dessart 1998) which mimic the spectral appearance of WR stars because their high luminosities drive dense and fast winds (Graefener & Hamann 2008).

If it is true that the most massive stars can be found in the most massive clusters (Bate 2002; Weidner & Kroupa 2006), then it can be expected that the most massive

---

⋆ E-mail: o.schnurr@sheffield.ac.uk

WN5-7ha stars are hosted by the most massive among the youngest, least evolved clusters known. NGC3603 is a Galactic example of such a cluster, and virtually a clone of its more famous LMC counterpart, the supermassive cluster R136, at the core of the giant HII region 30 Dor (Moffat et al. 1994). NGC3603's very core, itself denoted HD 97950, contains three extremely luminous WN6ha stars (Drissen et al. 1995), with stellar luminosities well in excess of 10^6 $L_\odot$ (de Koter et al. 1997; Crowther & Dessart 1998). Moffat & Niemela (1984) found from radial-velocity variations in unresolved spectra of HD 97950 that one of these WN6ha stars must be a binary with a period of 3.772 days, which was confirmed by Moffat et al. (1985). In a recent study, Moffat et al. (2004) used HST-NICMOS J-band photometry to confirm that A1 is indeed a double-eclipsing binary with that period, while the other WN6ha stars B and C did not vary above the ∼ 0.05 mag noise level. However, star C shows an extremely large X-ray luminosity (L_x = several 10^{34} ergs^{-1}; Moffat et al. 2002), which is a strong indication of binarity given that colliding winds in binary systems generate copious amounts of hard X-rays (e.g. Usov 1992).

The double-eclipsing nature of A1 offers the rare opportunity to directly measure the mass of an extremely luminous binary system by simple, least model-dependent Keplerian orbits. Here we report the results of a spectroscopic monitoring campaign of the three central WN6ha stars in NGC3603. This Letter is organized as follows: In Section 2, we briefly describe the observations and data reduction. In Section 3, data analysis is described and results are presented. Section 4 summarizes the Letter.

2 OBSERVATIONS AND DATA REDUCTION

Observations were carried out in service mode at the VLT-UT4 under Program-ID P75-0576.D. We obtained repeated K-band (1.95 to 2.45 μm) spectroscopy using SINFONI (Eisenhauer et al. 2003; Bonnet et al. 2004) with adaptive-optics (AO) correction to obtain the highest possible spatial and spectral resolution. The field of view was $0.8'' \times 0.8''$ with a "spaxel" scale of 12.5 mas × 25 mas. Each of our three target WN6ha stars was observed individually.

Total exposure times were 84s per star and per visit, each organized in 4 detector integration times (DITs) of 21s. Given the brightness of our targets ($K \sim$ 7–8mag) and the AO deployment, no dedicated sky frames were taken. Other calibrations (dark and flatfield frames, and the telluric standard star) were provided by the ESO baseline calibration.

For most of the data reduction steps, ESO's pipeline was used (cf. Abuter et al. 2006). Standard reduction steps were taken. The two-dimensional spectra produced by each illuminated slitlet were individually extracted using IRAF, and combined into one wavelength-calibrated spectrum per star and visit. A main-sequence B-type star was used for telluric corrections. To remove the B star's Brγ absorption which coincides with the Brγ/HeI λ2.166 μm emission blend of the target WN6ha stars, a Lorentzian was fitted to the absorption line and subtracted from the B star's spectrum. Residuals were very small, and proved to be harmless in the subsequent analysis. Finally, science spectra were rectified by fitting a low-order spline function to the stellar continuum. The final uniform stepwidth of the spectra was 2.45 Å/pixel, resulting in a conservative three-pixel resolving power of ∼3000, and a velocity dispersion of ∼33 kms^{-1}/pixel.

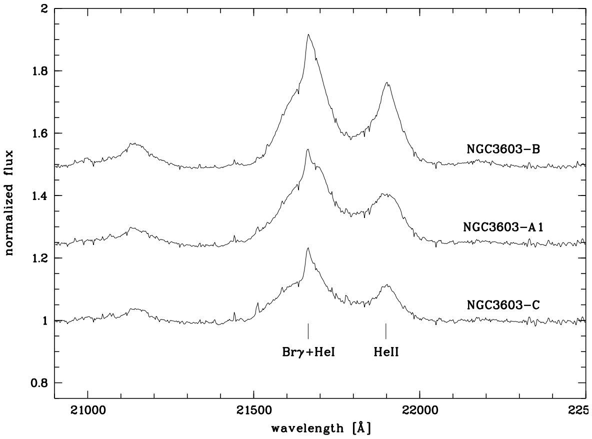

Figure 1. Montage of average spectra of our three target stars, limited to the useful spectral region. The two strongest emission lines, Brγ/HeI λ2.166 μm and HeII λ2.188 μm are indicated. For clarity, the upper two spectra have been shifted by 0.25 and 0.5 flux units, respectively.

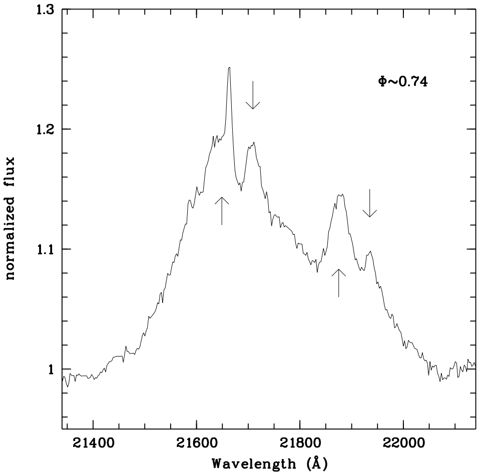

Figure 2. Average of two spectra of A1, taken almost at quadrature ($\phi \sim 0.74$). Both Brγ/HeI λ2.166 μm and HeII λ2.188 μm are clearly separated; the (stronger-lined) primary is indicated by upward arrows, while the (slightly weaker-lined) secondary is indicated by downward arrows.

3 DATA ANALYSIS AND RESULTS

Averaged spectra of the three WN6ha stars are shown in Figure 1. For star B, radial velocities (RVs) were measured by cross-correlation of the region 21340 to 22140 Å, comprising the two emission lines Brγ/HeI λ2.166μm and HeII λ2.188μm. Star B proved to show constant RVs over the observed timescales, with a scatter of $\sigma_\mathrm{RV} \sim 20$ kms^{-1}, which was adopted as *a-posteriori* error (see Figure 4). Fitting a

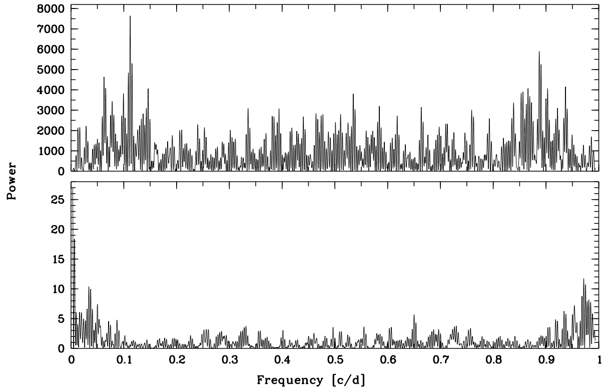

Figure 3. Power spectrum (upper panel) and spectral window (lower panel) for star C. Frequencies were searched from 0.1 to 1 d−1, corresponding to periods between 1 and 10 days. The strongest frequency peak at $\nu \sim 0.112$ d^{-1} corresponds to the adopted period of 8.89 days.

single Gaussian to the HeII $\lambda 2.188\mu$m emission line yielded a slightly larger scatter, $\sigma = 26$ kms^{-1}, but was used to obtain the systemic velocity of the star, $\gamma = (167 \pm 6)$ kms^{-1}. Given is the error of the mean, i.e. $\sigma/\sqrt(N)$, where $N = 18$ is the number of data points.

A1 was found to consist of two emission-line stars, very similar to WR20a (Rauw et al. 2004). An average spectrum around quadrature ($\phi \sim 0.74$) is shown in Figure 2. While both binary components show Brγ/HeI $\lambda 2.166\mu$m and HeII $\lambda 2.188\mu$m in emission, the two components do not show the same line strengths. In the following, we will hence refer to the stronger-lined star as "primary", and to the weaker-lined star as "secondary".

RVs for star C and for both components of A1 were obtained by independently fitting Gaussians to the respective HeII $\lambda 2.188\mu$m emission peaks of the two components, because this line is most likely less affected by wind-wind collision in the binary than Brγ/HeI. To take into account that in the case of A1, the HeII emission peak of the secondary moves up and down the flank of the stronger emission of the primary, a sloping, linear continuum was simultaneously fitted. Unfortunately, fitting the secondary's emission peaks in A1 is only possible at phases were the respective HeII lines are well separated, and particularly difficult when the weak HeII line of the secondary blends with the strong Brγ/HeI line of the primary, i.e. during most of the "blue" half-wave of the companion's motion. Moreover, due to blending with the steep slope of the Brγ/HeI emission, the profile of the secondary's HeII emission line gets significantly distorted, thereby further increasing the error of the fit. Both phenomena strongly affect the determination of the secondary's orbit and hence the mass determination of the two stars (see below). RVs for both components of A1 are listed in Table 1, and RVs for the primary component of C are listed in Table 2.

For star C, RVs were subjected to a period search based on the CLEAN algorithm and Scargle periodograms (see Schnurr et al. 2008 for details). The search yielded a value of $P = 8.89 \pm 0.01$ days (see Figure 3).

Orbital solutions for A1 and C were fitted to the RVs using ELEM (Marchenko et al. 1994) and applying $1/\sigma^2_{\rm RV}$ weights to the RVs. For star A1, the period reported by Moffat et al. (2004), $P = 3.7724$ d, was adopted, and for both A1 and C the orbital periods were fixed. In A1, RVs of both the primary and the secondary were fitted simultaneously, forcing a circular orbit and the systemic velocity to be the same for both components. While emission lines in WR stars are well known to display some degree of redshift with respect to the true systemic velocity of the star (see e.g. Schnurr et al. 2008), both WR components in A1 will display the same amount of redshift. Our approach is further justified by the fact that all three stars A1, B, and C show comparable systemic velocities.

Table 1. Journal of RVs for both components in A1 as obtained by Gaussian fits to the HeII $\lambda 2.188\mu$m emission lines. The second column of each table provides the orbital phase corresponding to a period of $P = 3.7724$ days (from Moffat et al. 2004) and, as zero point in phase, the time of inferior conjunction $E_0 = 2,453,765.75$ (this work). Note that it was not always possible to measure the RVs for the secondary; see text for more details.

HJD	ϕ	RV_1	σ_1	RV_2	σ_2
2,450,000.5+			kms^{-1}		
3468.003	0.206	475	7	-121	21
3470.030	0.743	-138	16	601	7
3471.060	0.016	262	7	262	9
3472.019	0.270	478	4	-267	55
3473.009	0.533	6	4		4
3474.146	0.834	-160	7	427	7
3489.970	0.029	305	7	305	8
3528.976	0.369	410	8		
3529.978	0.635	-45	10	531	55
3531.040	0.916	48	10		
3532.961	0.425	236	14	236	14
3552.963	0.727	-184	7	630	7
3721.321	0.356	426	7	21	27
3723.325	0.888	-121	27	210	21
3754.240	0.083	281	7		
3758.243	0.144	285	21		
3763.292	0.482	55	14	277	7
3765.213	0.991	177	7	177	8
3766.362	0.296	485	21	-40	41
3790.163	0.605	19	14		
3794.101	0.649	-125	7	499	21
3794.212	0.679	-100	21	507	21

Due to the low quality of the secondary's RV determination during the "blue" half-wave of its orbital motion, the fit of the secondary's orbit is dominated by the "red" half-wave. This leads to a large RV amplitude for the secondary and, by consequence, a large mass ratio. A significantly smaller RV amplitude would have been obtained if the systemic velocity of the secondary were left as a free fitting parameter. However, given the problems with the 'blue half-wave described above, we believe that it is more sensible to rely on the red half-wave with the smaller error bars and fix the systemic velocity.

Orbital fits for A1 and C are shown in Figure 4; the respective orbital parameters are given in Tables 3 and 4. Combining the orbital parameters of both components of A1 with the inclination angle obtained by Moffat et al. (2004), $i = 71°$, and using the usual relations, we obtain absolute masses of $M_1 = (116 \pm 31)$ $M_\odot$ for the primary and $M_2 = (89 \pm 16)$ $M_\odot$ for the secondary component of A1,

Table 2. As for Table 1, but for star C, using the period of $P = 8.89$ days and, as zero point for the phase, the time of periastron passage $T_0 = 2,453,547.11$ (this work).

HJD 2,450,000.5+	ϕ	RV	$\sigma_{\rm RV}$
		kms^{-1}	
3467.994	0.157	394	4
3468.003	0.158	425	8
3470.021	0.385	255	5
3471.060	0.502	93	7
3472.019	0.609	114	7
3473.009	0.721	-5	11
3474.146	0.849	0	10
3489.970	0.629	108	8
3528.976	0.016	263	10
3529.978	0.129	401	4
3531.040	0.249	381	10
3532.961	0.465	233	4
3552.963	0.715	19	7
3721.321	0.652	52	4
3723.325	0.878	-5	11
3754.240	0.355	216	4
3758.243	0.806	-21	8
3759.369	0.932	179	14
3763.292	0.374	244	14
3765.213	0.590	89	27
3766.353	0.718	45	11
3766.362	0.719	34	11
3769.387	0.059	293	12
3790.164	0.396	255	11
3791.102	0.502	110	18
3794.101	0.839	-27	14
3794.212	0.852	21	11

Table 3. Orbital parameters for both the primary and the secondary component of A1 from the combined, weighted fit, forcing a circular solution. The inclination angle and the period have been adopted from Moffat et al. (2004).

Parameter	Primary	Secondary
P [days]	3.7724	
i [°]	71	
e	0	
E_0 [2,450,000.5+]	3765.25 ± 0.03	
γ [kms^{-1}]	153 ± 12	
K [kms^{-1}]	330 ± 20	433 ± 53
$\sigma_{\rm o-c}$ [kms^{-1}]	42	82
M [$M_\odot$]	116 ± 31	89 ± 16

respectively. Due to the problems with the secondary's RVs described above, the uncertainties on the orbits, expressed by the large $\sigma_{\rm o-c}$, and hence on the masses are uncomfortably large. However, Drissen et al. (1995) have reported an absolute magnitude of $M_{\rm V} = -7.5$ for A1, i.e. brighter by ~ 0.5 mag than WR20a, for which Rauw et al. (2007) find $M_{\rm V} = 7.04 \pm 0.25$. Since A1 and WR20a have very similar spectral types and, thus, bolometric corrections, A1's brighter magnitude directly translates into a larger bolometric luminosity, qualitatively consistent with our result that A1 is more massive than WR20a. However, better data are currently being taken to verify the results.

Table 4. Orbital parameters for the WN6ha (primary) component in star C.

Parameter	Primary
P [days]	8.89 ± 0.01
e	0.30 ± 0.04
ω [°]	281 ± 7
T_0 [2,450,000.5+]	$3{,}546.61 \pm 0.18$
γ [kms^{-1}]	186 ± 6
K [kms^{-1}]	200 ± 23
$\sigma_{\rm o-c}$ [kms^{-1}]	27

In star C, the secondary is not visible in the spectrum; hence, we temporarily classify the system as SB1. While the intrinsic brightness difference between A1 and C is ~ 0.5 mag (Crowther & Dessart 1998), it is well possible that the WN6ha component in C is as massive as the primary in A1, where the luminosities of the primary and secondary are more similar; for the same reason, a large mass ratio can be expected between the primary and secondary component in C.

Star B, on the other hand, displays neither significant RV nor photometric variations (cf. Moffat et al. 2004) nor a strong X-ray flux. The latter is a strong indication against B's possible long-period binarity. Therefore, B most likely is a truly single star. Remarkably, Crowther & Dessart (1998) report a luminosity for B which is only very slightly lower than that of the (unresolved) system A1. This renders B significantly more massive than the primaries in both A1 and C, and puts it close to (or even in excess of) the putative IMF cut-off mass, unless B turns out to be an unresolved, long-period binary as well. Clearly, line-blanketed atmosphere models will provide valuable insights into this problem once the known, very massive binary systems such as A1 and WR20a have been used as yardsticks.

4 SUMMARY AND CONCLUSION

We have obtained repeated, spatially resolved, AO assisted, near-IR spectroscopy of the three central WN6ha stars in HD 97950, the core of the young, unevolved and very massive Galactic cluster NGC3603. One of the stars, A1, is a previously known, double-eclipsing binary with an orbital period of 3.77 days (Moffat & Niemela 1984; Moffat et al. 1985; Moffat et al. 2004), while a second star, C, was newly identified as a binary in the present study. The third star, B, showed constant RVs over the observed time interval, and therefore is most likely not a binary, which is in line with its normal X-ray luminosity (Moffat et al. 2002).

While in star C only the primary (WN6ha) component is visible – the system is therefore classified as an SB1 binary –, A1 consists of two emission-line stars, most likely of similar, but hot identical spectral types. From the radial-velocity curves of the two components and the known inclination angle of the system (Moffat et al. 2004), we derived component masses of $M_1 = (116 \pm 31)M_\odot$ for the primary and $M_2 = (89 \pm 16)M_\odot$ for the secondary, respectively. Despite the large uncertainties, we consider the primary WN6ha component of A1 to be the most massive star ever directly weighed.

While the primary component of C might have a mass similar to or even greater than that of A1's primary, it is possible that star B, single yet only slightly fainter than the combined binary system A1, is indeed the most massive member in NGC3603 and, therefore, the most massive main-sequence star known in the Galaxy.

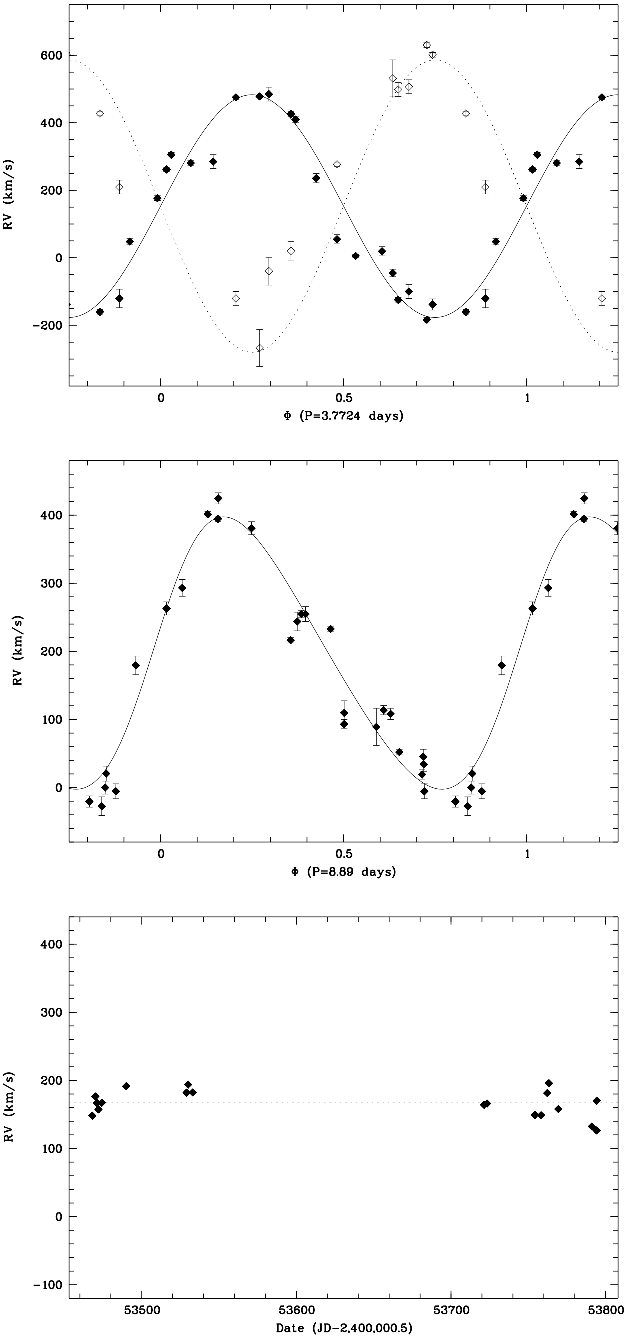

Figure 4. Orbital solutions obtained from weighted fits for A1 (upper panel) and C (middle panel), folded in the respective phases. In A1, the primary is indicated by filled symbols and the solid curve, while the secondary is shown with open symbols and the dotted curve. In star C, only the primary is visible. RVs of star B are constant during the observations (lower panel, same scale as for star C) with a scatter of $\sigma = 20$ kms^{-1} . The dashed line indicates the systemic velocity of the star B, $\gamma = (167 \pm 6)$ kms^{-1}.

REFERENCES

Abuter R., Schreiber J., Eisenhauer F., Ott T., Horrobin M., Gillesen S., 2006, New Astronomy Review, 50, 398

Bate M. R., 2002, in Shara M. M., ed., ASPC 263, 111

Bonanos A. Z., Stanek K. Z., Udalski A., Wyrzykowski L., Żebruń K., Kubiak M., Szymański M. K., Szewczyk O., Pietrzyński G., Soszyński I., 2004, ApJ, 611, L33

Bonnet H., Abuter R., Baker A., Bornemann W., et al., 2004, The Messenger, 117, 17

Crowther P. A., Dessart L., 1998, MNRAS, 296, 622

de Koter A., Heap S. R., Hubeny I., 1997, ApJ, 477, 792

Drissen L., Moffat A. F. J., Walborn N. R., Shara M. M., 1995, AJ, 110, 2235

Eisenhauer F., Abuter R., Bickert K., Biancat-Marchet F., et al., 2003, in Iye M., Moorwood A. F. M., eds., Proc. SPIE, 4841, 1548

Figer D. F., 2005, Nat, 434, 192

Gamen R., Barba R., Morrell N., Arias J., Maiz Apellaniz J., Sota A., Walborn N. R., Alfaro E., 2008, ArXiv e-prints, 803

Graefener G., Hamann W. ., 2008, ArXiv e-prints, 803

Lamontagne R., Moffat A. F. J., Drissen L., Robert C., Matthews J. M., 1996, AJ, 112, 2227

Marchenko S. V., Moffat A. F. J., Koenigsberger G., 1994, ApJ, 422, 810

Massey P., Penny L. R., Vukovich J., 2002, ApJ, 565, 982

Moffat A. F. J., Corcoran M. F., Stevens I. R., Skalkowski G., Marchenko S. V., Mücke A., Ptak A., Koribalski B. S., Brenneman L., Mushotzky R., Pittard J. M., Pollock A. M. T., Brandner W., 2002, ApJ, 573, 191

Moffat A. F. J., Drissen L., Shara M. M., 1994, ApJ, 436, 183

Moffat A. F. J., Niemela V. S., 1984, ApJ, 284, 631

Moffat A. F. J., Poitras V., Marchenko S. V., Shara M. M., Zurek D. R., Bergeron E., Antokhina E. A., 2004, AJ, 128, 2854

Moffat A. F. J., Seggewiss W., Shara M. M., 1985, ApJ, 295, 109

Nakamura F., Umemura M., 2001, ApJ, 548, 19

Rauw G., De Becker M., Nazé Y., Crowther P. A., Gosset E., Sana H., van der Hucht K. A., Vreux J.-M., Williams P. M., 2004, A&A, 420, L9

Rauw G., Manfroid J., Gosset E., Nazé Y., Sana H., De Becker M., Foellmi C., Moffat A.F.J., 2007, A&A, 463, 981

Schaerer D., 2002, A&A, 382, 28

Schnurr O., Moffat A. F. J., St-Louis N., Morrell N. I., Guerrero M. A. R., 2008, MNRAS, submitted

Usov V. V., 1992, ApJ, 389, 635

Weidner C., Kroupa P., 2004, MNRAS, 348, 187

Weidner C., Kroupa P., 2006, MNRAS, 365, 1333